Theor Chem Acc (2006) 115: 170–176
DOI 10.1007/s00214-005-0050-8

REGULAR ARTICLE

**Andrei V. Egorov · Andrei V. Komolkin**
**Alexander P. Lyubartsev · Aatto Laaksonen**

# First and second hydration shell of $Ni^{2+}$ studied by molecular dynamics simulations

Received: 31 May 2005 / Accepted: 23 September 2005 / Published online: 6 January 2006


**Abstract** Molecular dynamics simulations of a $Ni^{2+}$ ion in water have been carried out to investigate the structure and dynamics of water molecules around the nickel, extending the analysis to the second hydration shell. The structural parameters as well as the motions of water molecules in various sub-structures of the solution have been evaluated giving a detailed picture of the motional modes of water molecules.

**Keywords** Nickel cation · Hydration · Molecular dynamics simulation

## 1 Introduction

During the last decades the structure and dynamics of the hydration complexes of the nickel cation has been studied extensively using various experimental and theoretical methods [1–8]. Structural, dynamical and other properties of aqueous solutions of nickel salts have also been a subject of several comprehensive reviews [9–11]. Although a considerable amount of work has been devoted to interpret the experimental data in terms of molecular structures and motions, a detailed molecular-level description of water structure and dynamics around the nickel cation is still largely missing. In this context, computer simulations, capable to provide detailed information of all the atoms in the simulated systems on a nanosecond time-scale, should be very helpful for further investigation of this problem. However, it should be kept in mind that any classical computer simulation is always as good as the used potential model describing the interactions between the molecules.

In ab initio simulations the forces are determined directly from quantum chemical calculations without any interaction potentials. It is therefore tempting to expect that these types of simulations are more reliable than classical molecular dynamics simulations. However, quantum chemical or ab initio simulations are computationally very expensive and, therefore, provide only a limited statistical sampling. Typically, only a few tens of picoseconds can currently be covered by Car–Parrinello Molecular Dynamics (MD) where the number of water molecules, feasible to include, is normally less than 100. In hybrid QM/MM simulations the size of the system can be increased to same order as used in standard classical MD simulations and time can be prolonged from what is typical for Car–Parrinello simulations. Still, it is not enough to provide reliable results for transport properties.

In the case of $Ni^{2+}$ in aqueous solutions, both classical MD or Monte Carlo (MC) computer simulation studies [12–23] report a very broad range of results, obtained with different ion–water potential models (see Table 1). Surprisingly quite a little attention has been paid to the molecular mechanisms behind the hydration water motion in nickel solutions. The analysis of the librational and vibrational motions of water as well as the possible water-exchange mechanism has been reported by Inada et al. [20,21]. The dynamics of the $Ni^{2+}$ hexa-aquo complex was studied by Westlund et al. [13] and Odelius et al. [15,16]. However, these works were aimed mainly at the simulation of NMR relaxation. Therefore they did not consider the second hydration shell at all. Moreover, the ion–water potential used by Westlund et al. [13] was initially constructed to describe $Mg^{2+}$–water interactions.

In the present study the aqua-complex of nickel cation has been treated by MD method without any constraints in order to analyse the structure and dynamics as well as molecular mechanisms of water substitutions and exchange in the first and second shells around the divalent cation.

## 2 Methods

### 2.1 Interaction potential models

In computer simulations the choice and evaluation of the interaction potentials is always a mandatory prerequisite for

A.V. Egorov · A.V. Komolkin
Institute of Physics, St. Petersburg University, 198504, St. Petersburg, Russia

A.P. Lyubartsev · A. Laaksonen (✉)
Division of Physical Chemistry, Arrhenius Laboratory, Stockholm University, Stockholm, 106 91, Sweden
E-mail: aatto@physc.su.se

**Table 1** An overview of results from earlier nickel cation hydration simulations. $T$: temperature, $r_{NiO}^{1\,max}$ and $r_{NiH}^{1\,max}$: positions of the Ni–O and Ni–H radial distribution function first maximum, $N_{Ni}$: cation coordination number, $D_{Ni}$: self-diffusion coefficient

| Method | System | Water model | $Ni^{2+}$–water potential | $T$(K) | $r_{NiO}^{1\,max}$, (Å) | $r_{NiH}^{1\,max}$, (Å) | $N_{Ni}$ | $D_{Ni}$, ($10^{-9}$ m$^2$/sec) | Ref. |
|---|---|---|---|---|---|---|---|---|---|
| MD-NVE | 1 Ni:64 $H_2O$ | TIP4P | 2-body | 316 | 2.17 | 2.76 | 8.0 | | [12] |
| MD-NVT | 1 Ni:215 $H_2O$ | $SPC_{flex}$ | 2-body | 298 | 1.96 | 2.69 | 6.0 | 0.18 | [13] |
| MC-NVT | 1 Ni:200 $H_2O$ | MCY | 2-body | 298 | 2.09 | 2.75 | 8.0 | | [14] |
| | | | 3-body | | 2.07 | 2.69 | 6.0 | | |
| MD-NVT | 1 Ni:255 $H_2O$ | SPC/E | 2-body | 300 | 2.056 | 2.67 | 6.0 | 0.82 | [15,16] |
| MD-NVT | 2 $NiBr_2$:278 $H_2O$ | SPC/E | 2-body | 298 | 2.068 | | 6.0 | | [17,18] |
| MD-NVT | 30 $NiCl_2$:1,282 $H_2O$ | SPC/E | 2-body | 298 | 2.06 | 2.75 | 4.5 | | [19] |
| | | | | 373 | | | 4.5 | | |
| MD-NVT | 1 Ni:499 $H_2O$ | BJH | 2-body | 298 | 2.15 | | 8.0 | | [20,21] |
| MD-NVT | | | 3-body | | 2.25 | | 6.0 | | |
| MC-NVT | | | 2-body | | 2.15 | | 8.0 | | |
| MC-NVT | | | 3-body | | 2.21 | | 6.0 | | |
| QM/MM-NVT | | | 3-body | | 2.14 | | 6.0 | | |
| MD-NVT | 1 Ni:819 $H_2O$ | SPC/E | 2-body | 300 | 2.07 | 2.76 | 6.0 | | [22,23] |

a reliable description of the investigated system. In the case of nickel cation there is a lack of good quality 2-body ion–water potentials. Concerning the interaction potentials between water and nickel cation in general, Inada et al. [20, 21] did postulate that the inclusion of 3-body corrections is necessary to reproduce correctly the peculiarities of $Ni^{2+}$ hydration in classical simulations. However, this claim may be too categorical. Recently, an effective 2-body $Ni^{2+}$–water interaction potential, given in a following functional form:

$$
\begin{aligned}
V(r) = {} & \frac{q_{Ni}q_O}{r_{NiO}} + \frac{A_O}{r_{NiO}^4} + \frac{B_O}{r_{NiO}^6} + \frac{C_O}{r_{NiO}^8} + \frac{D_O}{r_{NiO}^{12}} \\
& + E_O \cdot \exp(-F_O r_{NiO}) \\
& + \sum_{H=H_1,H_2} \frac{q_{Ni}q_H}{r_{NiH}} + \frac{A_H}{r_{NiH}^4} + \frac{B_H}{r_{NiH}^6} \\
& + \frac{C_H}{r_{NiH}^8} + \frac{D_H}{r_{NiH}^{12}},
\end{aligned}
$$

has been proposed based on ab initio studies [22,23]. Parameters used in this potential are collected in Table 2.

**Table 2** Parameters of the nickel–water interaction potential from Refs. [22,23]

| Parameter | Value |
|---|---|
| $A_O$ | $-3.861\times10^3$ kJ mol$^{-1}$ Å$^4$ |
| $B_O$ | $6.985\times10^4$ kJ mol$^{-1}$ Å$^6$ |
| $C_O$ | $-8.618\times10^4$ kJ mol$^{-1}$ Å$^8$ |
| $D_O$ | $3.538\times10^4$ kJ mol$^{-1}$ Å$^{12}$ |
| $E_O$ | $-6.686\times10^4$ kJ mol$^{-1}$ |
| $F_O$ | 2.4077Å$^{-1}$ |
| $A_H$ | $1.119\times10^3$ kJ mol$^{-1}$ Å$^4$ |
| $B_H$ | $-8.688\times10^2$ kJ mol$^{-1}$ Å$^6$ |
| $C_H$ | $-1.677\times10^3$ kJ mol$^{-1}$ Å$^8$ |
| $D_H$ | $9.748\times10^2$ kJ mol$^{-1}$ Å$^{12}$ |

This interaction potential has been employed in classical MD simulations [22,23] where it succeeds to reproduce the very same nickel–water radial distribution functions as were obtained from X-ray spectroscopy. The SPC/E water model [24] was used in the nickel–water potential fitting procedure. We have chosen to use this model in our simulations.

### 2.2 Computational details

The simulations of one $Ni^{2+}$ ion among 255 water molecules (0.214 mol/kg solution) in a cubic periodic cell were carried out in a canonical NVT ensemble at 25°C. The density of simulation box was set to be equal 0.997 g/cm$^3$. Temperature was kept constant by using the Nosé–Hoover method [25,26]. The equations of motion were solved using the standard Verlet leap-frog algorithm with a time step of 1.0 fs. The long-range Coulomb forces are calculated using the Ewald summation method. The simulated system is obviously not electro-neutral but this fact does not affect the properties calculated in this work. Counter-ions like $Cl^-$ are not included because they are expected to disturb the hydration structure. The configuration was equilibrated during a 150 ps run. Finally, a 1.5 ns simulation was performed.

## 3 Results and discussion

### 3.1 Hydration structure

Experiments [1,3,4,9] suggest that $Ni^{2+}$ ion coordinates six water molecules. This complex is stable over a range of microseconds [2,10,11]. Our MD simulations reproduce the very same structural picture. Calculated nickel–water radial distribution functions (not displayed) nicely coincide with the recent results obtained from X-ray absorption fine structure

[22,23] and the cation coordination number calculated from them equals to 6.0.

A detailed view on the structure of $Ni^{2+}$ hydration shells can be given using various density maps of water oxygen and hydrogen distributions relative to nickel cation. Special density projection maps (cylindrical distribution functions or CDFs) are shown in Figs. 1 and 2. These density maps show distributions of water oxygen and hydrogen atoms relative to nickel ion together with another water oxygen in the first hydration shell. In the computation of CDFs, the local $Z$-axis is pointed along the vector connecting the $Ni^{2+}$–O pair. Space around is divided into cylindrical segments with steps of 0.1 Å in both dimensions. The local density is then given as a properly normalized number of atoms in each segment. In the CDFs we have plotted the ratio of local density to bulk density as a scale of greys (see Figs. 1, 2). Combined oxygen and hydrogen distribution in the first and second hydration shells are presented in Fig. 3 as iso-density spatial distribution functions. The octahedral structure of the nickel coordination is very well pronounced. We can see from Fig. 3 that six water oxygens (green) are arranged around nickel. These water molecules are free to rotate around their dipole axis. The two hydrogens of the water molecules are found in the donut-shaped density (shown red). The green rings on top of the red rings are oxygens from the second hydration. Only two of them are shown for clarity. The number of water molecules in the second shell is calculated to be equal to 12.9.

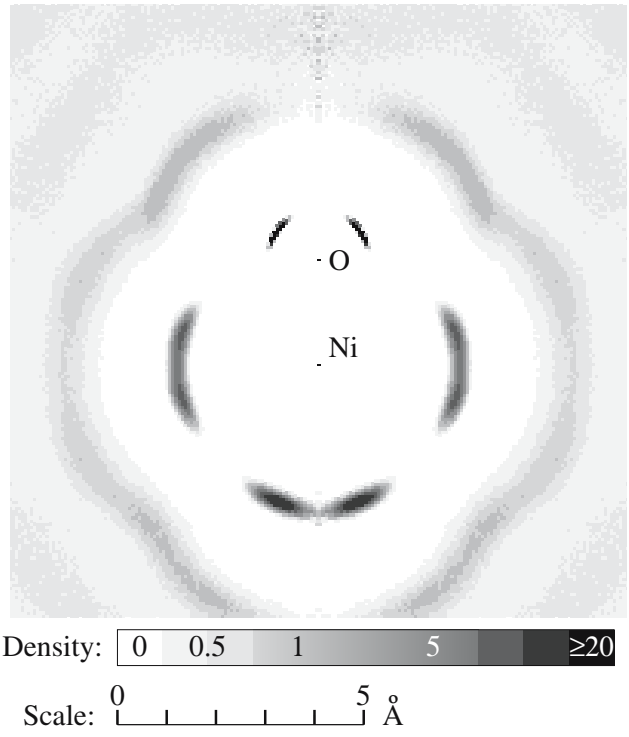


**Fig. 2** Calculated distribution of water hydrogen density around a fixed Ni–O pair

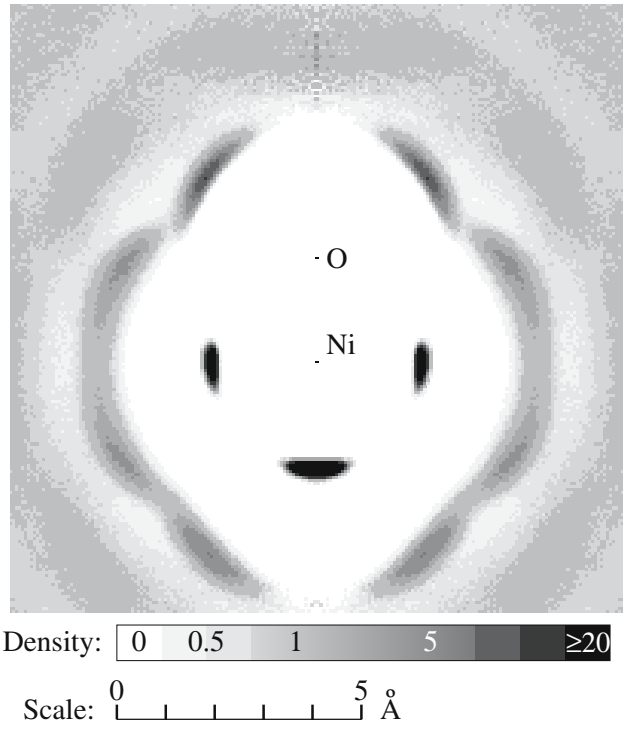


**Fig. 1** Calculated distribution of water oxygen density around a fixed Ni–O pair

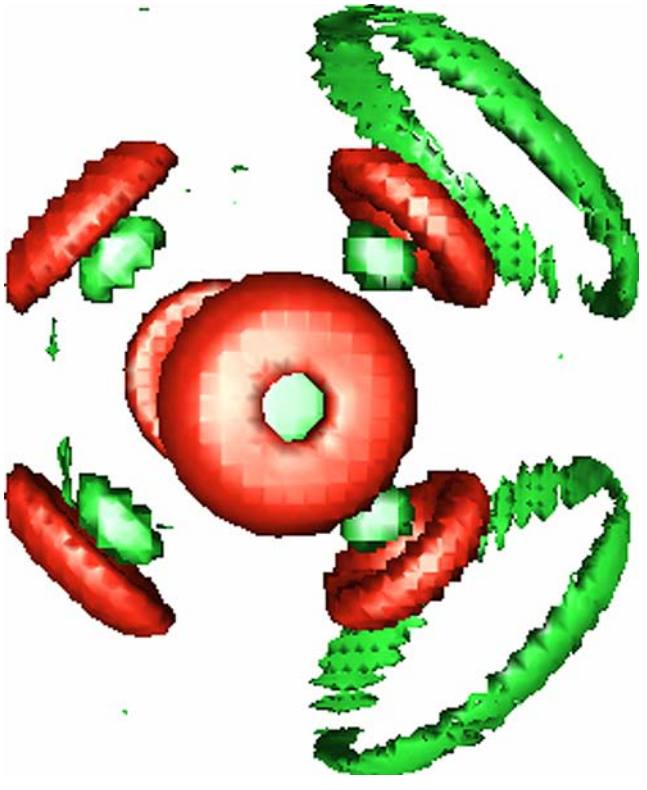

**Fig. 3** Spatial distribution functions of water oxygen (green) and hydrogen (red) around the $Ni^{2+}$ cation. The density threshold is five times the bulk density

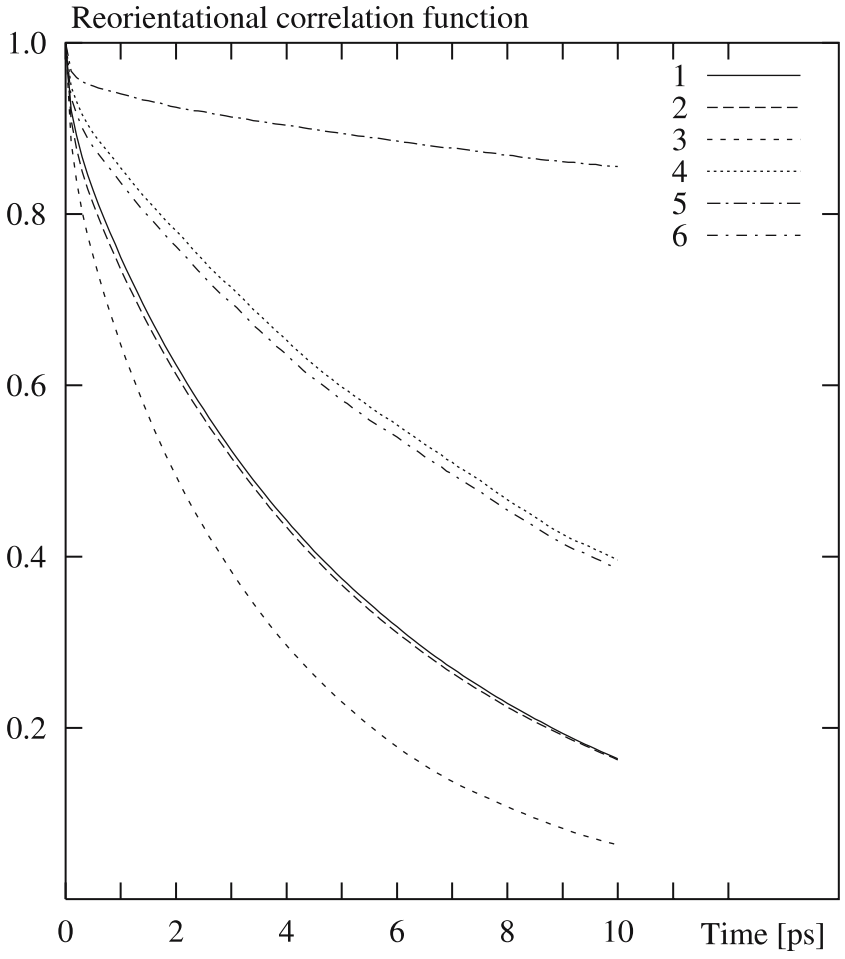


**Fig. 4** First rank reorientational time correlation functions for water molecules. Bulk water: 1 – $\mathbf{R}_{HH}$, 2 – $\mathbf{R}_D$, and 3 – $\mathbf{R}_P$ vectors. The first hydration shell: 4 – $\mathbf{R}_{HH}$, 5 – $\mathbf{R}_D$, and 6 – $\mathbf{R}_P$ vectors

### 3.2 Dynamical behaviour

The residence times of water molecules in the nickel hydration shells are calculated following the standard procedure described in Ref. [27]. No exchange of the $Ni^{2+}$ first hydration shell water molecules was observed during the whole 1.5 ns simulation run. The average residence time for water molecules in the second coordination shell is 9.5 ps. This is very close to the 10.3 ps value obtained by Chillemi et al. [23] in their MD simulations.

The nickel–cation self-diffusion coefficient was also computed from the mean square displacements of the molecules. The MD result – $0.65\times10^{-9}$ $m^2/s$, agrees well with the experimental value $0.671\times10^{-9}$ $m^2/s$ measured for 0.2 mol/L $NiCl_2$ aqueous solution by diaphragm cell method [28].

A detailed view on the water dynamics around $Ni^{2+}$ can be given through the reorientational correlation functions, $C_l^\alpha = \langle P_l(\mathbf{e}^\alpha(t)\cdot\mathbf{e}^\alpha(0))\rangle$, where $P_1$ and $P_2$ are the first and second rank Legendre polynomials, respectively, and $\mathbf{e}^\alpha$ is the unit vector pointed along the $\alpha$ axis in the molecular frame of each water molecule. The correlation time, $\tau_l^\alpha$, can be obtained by fitting the correlation functions using the following expression: $C_l^\alpha = e^{-t/\tau_l^\alpha}$. In our analysis we have used three different axes: the H–H vector, $\mathbf{R}_{HH}$, the molecular dipole, $\mathbf{R}_D$, and the normal to the plane of the molecule, $\mathbf{R}_P$. The results are presented in Fig. 4 and Table 3.

In bulk water the correlation time of the $\mathbf{R}_P$ vector is shorter than the correlation times in the plane of the molecule. The same result was obtained in MD simulations of pure SPC/E water [29]. This anisotropy seems to be caused by the geometry of the water model. The dynamics of water molecules within the $[Ni(H_2O)_6]^{2+}$ complex changes completely. First of all, the correlations times are much longer. Secondly, the rotation around the molecular dipole vector becomes the dominant motion. It should be noted that similar dynamics is

**Table 3** Reorientational–rotational correlation times (in ps) for water molecules in various solution sub-structures around the nickel ion

| Vector | Bulk water | | The first shell | | The second shell | |
|---|---|---|---|---|---|---|
| | $\tau_1$ | $\tau_2$ | $\tau_1$ | $\tau_2$ | $\tau_1$ | $\tau_2$ |
| $\mathbf{R}_{HH}$ | 5.8±0.2 | 3.2±0.2 | 17±1 | 8.0±0.3 | 5.5±0.5 | 4.5±0.2 |
| $\mathbf{R}_D$ | 6.1±0.2 | 2.7±0.2 | 95±5 | 36±2 | 15±1 | 5.4±0.5 |
| $\mathbf{R}_P$ | 3.9±0.2 | 2.3±0.2 | 17±1 | 7.8±0.3 | 4.5±0.5 | 3.7±0.4 |

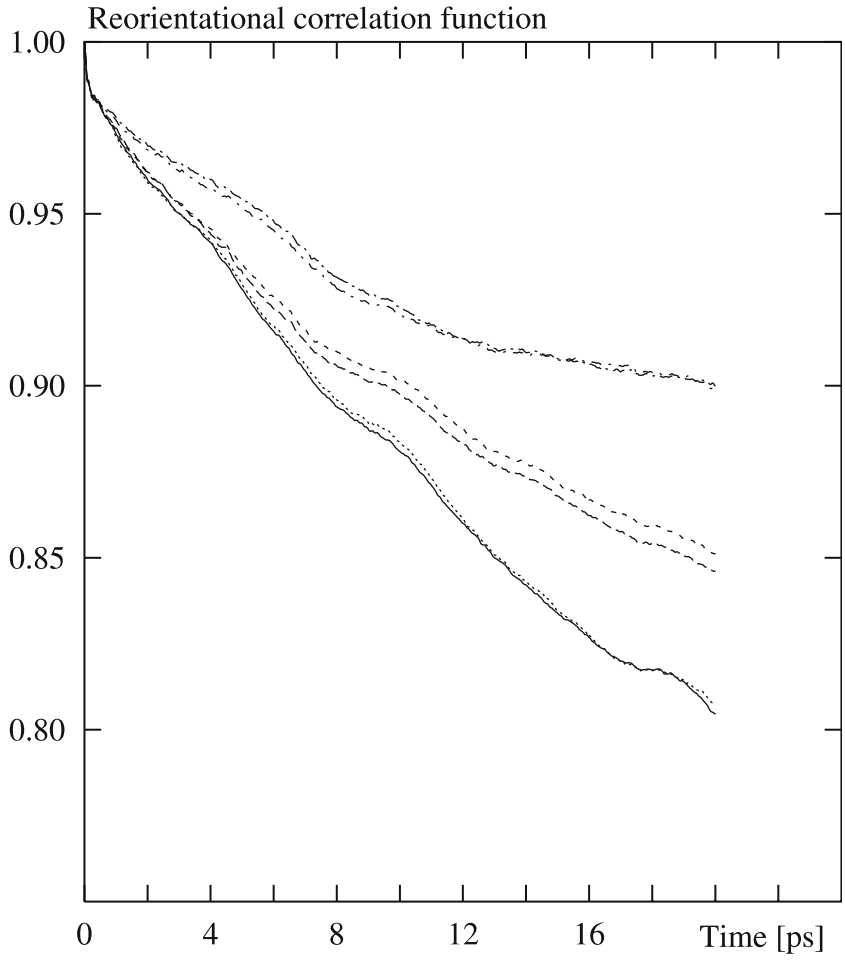


**Fig. 5** Six reorientational correlation functions for Ni–O vectors within the $[Ni(H_2O)_6]^{2+}$ complex

typical for water molecules even within the second hydration shell. Despite the frequent exchange with bulk water substructure, the reorientation of the $\mathbf{R}_D$ vector is the slowest motion.

Concerning the first shell the structure of nickel hexa-aquo complex is very stable. The six water molecules coordinating the $Ni^{2+}$ do not interchange their places within the shell during the 1.5 ns simulation. Therefore we can define the reorientational correlation time for the complex as a whole. The results are shown in Fig. 5. The correlation functions converge very slowly. The average correlation times $\tau_1$ and $\tau_2$ are about 150 and 40 ps correspondingly. Moreover, the correlation times for the O–Ni–O axes of the complex are different. It means that 1.5 ns simulation run is too short to describe correctly the $[Ni(H_2O)_6]^{2+}$ complex global reorientation.

Nevertheless, several well-pronounced instantaneous deviations (up to 50°–60°) of the complex axes were observed during the simulations. The analysis of this effect was carried out in the following way. The inner part of the second hydration shell was divided in 0.1 Å thick layers. Every 10 fs it was checked if a water oxygen or hydrogen atoms lie within the layers. An example of the evolution of the atoms positions within the inner part of the second hydration shell during a randomly selected interval of 10 ps from the entire run is presented in Fig. 6. The corresponding reorientational correlation functions for O–Ni–O axes within the $[Ni(H_2O)_6]^{2+}$ complex are also included. A well-pronounced correlation between the complex axes reorientation and the instantaneous oxygen movements towards the first hydration shell is observed. We can conclude that the main molecular mechanism of nickel hexa-aquo complex reorientation is due to the rapid pushes given by the second shell water oxygens. Those rotations of water molecules within the second shell, which only change the hydrogen positions do not affect the complex orientation.

## 4 Conclusions

In this paper an MD study of $Ni^{2+}$ cation hydration have been carried out. The structural parameters of the first and the second hydration shells as well as the motions of water molecules in various sub-structures of the solution were evaluated. The simulations showed that the structure of $[Ni(H_2O)_6]^{2+}$ complex is very stable and the reorientational correlation

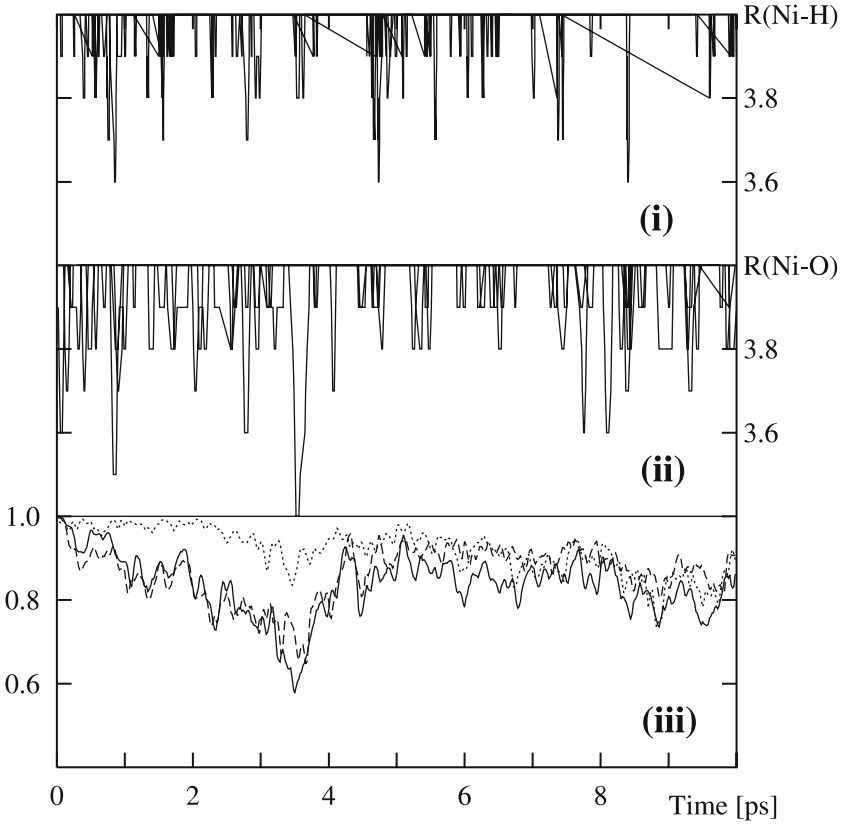


**Fig. 6** (i) The evolution of water hydrogens positions within the inner part of the second hydration shell. *R*(Ni–H) is the instantaneous distance between second shell-water hydrogens and nickel cation; (ii) the corresponding evolution of water oxygen positions within the inner part of the second hydration shell. *R*(Ni–O) is the instantaneous distance between second shell-water oxygens and nickel cation; (iii) corresponding reorientational correlation functions for O–Ni–O axes within the $[Ni(H_2O)_6]^{2+}$ complex

functions for the complex as a whole converge very slowly. The main molecular mechanism of the complex reorientation is the pushes given by the second shell water oxygens. The rotations of water molecules within the second shell, which change the hydrogens positions only, do not affect the complex orientation. It was also found that, despite the intensive exchange with bulk water, the dynamics of water molecules within the second hydration shell is like in the first one.

The results of present study represent a small step forward in the description of the peculiarities of nickel cation hydration and may be used in further investigations of NMR relaxation process in aqueous nickel solutions.

**Acknowledgements** We thank Dr. Giovanni Chillemi (CASPUR, Italy) for his valuable help. The financial support by the Russian Foundation for Basic Research (grant 04-03-32639), the Russian ministry of Education and Science (grant 37554), St. Petersburg Government (grant PD05-1.2-8), and the Swedish Science Council (VR) are gratefully acknowledged.

## References

1. Hunt JP, Friedman HL (1983) Prog Inorg Chem 30:359–387
2. Friedman HL (1985) Chem Scr 25:42–48
3. Neilson GW, Enderby JE (1996) J Phys Chem 100:1317–1322
4. Howell I, Neilson GW (1997) J Mol Liq 73–74:337–348
5. Rotzinger FP (1996) J Am Chem Soc 118:6760–6766
6. Friedman HL, Holz M, Hertz HG (1979) J Chem Phys 70:3369–3383
7. Ducommun Y, Earl WL, Merbach AE (1979) Inorg Chem 18:2754-2758
8. Kowalewski J, Larsson T, Westlund P-O (1987) J Magn Res 74:56–65
9. Ohtaki H, Radnai T (1993) Chem Rev 93:1157–1204
10. Helm L, Merbach AE (1999) Coord Chem Rev 187:151–181
11. Erras-Hanauer H, Clark T, van Eldik R (2003) Coord Chem Rev 238–239:233–253
12. Bounds DG (1985) Mol Phys 54:1335–1355
13. Westlund P-O, Larsson TP, Teleman O (1993) Mol Phys 78:1365–1384
14. Cordeiro MNDS, Ignaczak A, Gomes ANF (1993) Chem Phys 176:97–108
15. Odelius M, Ribbing C, Kowalewski J (1995) J Chem Phys 103:1800–1811
16. Odelius M, Ribbing C, Kowalewski J (1996) J Chem Phys 104:3181–3188
17. Wallen SL, Palmer BJ, Fulton JL (1998) J Chem Phys 108:4039–4046
18. Hoffmann MM, Darab JG, Palmer BJ, Fulton JL (1999) J Phys Chem A 103:8471–8482
19. Chialvo AA, Simonson JM (2002) Mol Phys 100:2307–2315
20. Inada Y, Mohammed AM, Loeffler HH, Rode BM (2002) J Phys Chem A 106:6783–6791
21. Inada Y, Loeffler HH, Rode BM (2002) Chem Phys Lett 358:449–458

22. D'Angelo P, Barone V, Chillemi G et al. (2002) J Am Chem Soc 124:1958–1967
23. Chillemi G, D'Angelo P, Pavel NV et al. (2002) J Am Chem Soc 124:1968–1976
24. Berendsen HJC, Grigera JR, Straatsma TP (1987) J Phys Chem 91:6269–6271
25. Nosé S (1984) Mol Phys 52:255
26. Martyna GJ, Tobias DJ, Klein ML (1994) J Chem Phys 101:4177–4189
27. Impey RW, Madden PA, McDonald IR (1983) J Phys Chem 87:5071–5083
28. Mills R, Lobo VMM (1989) Self-Diffusion in electrolyte solutions. Elsevier, Amsterdam
29. van der Spoel D, van Maaren PJ, Berendsen HJC (1998) J Chem Phys 108:10220–10230